Contribution of airbornegeophysicalimaging to the mapping of Birimian formations in the Kalamonmining permit, Bouna, Northeastern Côte d'Ivoire.

Résumé

La région de Kalamon, située dans le district minier de Bouna au Nord-Est de la Côte d'Ivoire, fait partie intégrante du domaine paléoprotérozoïque de la dorsale de Man (Craton Ouest-Africain). Dans ce secteur, la présence d'une couverture latéritique subcontinue et particulièrement épaisse (30 à 90 m) constitue un obstacle majeur à la cartographie directe des formations rocheuses.
La présente étude combine le traitement haute résolution de données géophysiques aéroportées (aéromagnétisme et spectrométrie gamma) et l'examen pétrographique détaillé d'échantillons de forages carottés pour cartographier et caractériser les essaims de dykes de dolérite traversant le permis minier de Kalamon.
L'analyse filtrée du champ magnétique total (réduction au pôle, signal analytique et première dérivée verticale) met en évidence des anomalies linéaires étroites et fortement magnétiques, d'orientations préférentielles N-S à NNE-SSW et NW-SE. L'examen microscopique révèle que ces intrusions basiques possèdent une texture ophitique à subophitique typique, dominée par l'enchevêtrement de lattes de plagioclase (labrador à bytownite) et d'augite, accompagnées d'une proportion notable d'oxydes de fer et de titane (magnétite titanifère et ilménite), responsables de la forte réponse aéromagnétique. Les transformations deutériques de bas grade s'illustrent par une uralitisation partielle des pyroxènes et une séricitisation des plagioclases. Ce couplage méthode géophysique/pétrographie démontre son efficacité pour reconstituer la géométrie des conduits magmatiques subvolcaniques et affiner le schéma géodynamique régional.

Mots-clés :Aéromagnétisme, Dykes, Pétrographie, Kalamon, Bouna, Craton Ouest-Africain.

Abstract

The Kalamon area, locatedwithin the Bouna mining district in northeastern Côte d'Ivoire, forms part of the Paleoproterozoicdomain of the Man Shield (West African Craton). In thissector, the presence of a subcontinuous and particularlythicklateritic cover (30 to 90 m) represents a major obstacle to direct geological mapping. This study combines high-resolutionairbornegeophysical data processing (aeromagnetics and gamma-ray spectrometry) withdetailedpetrographicexamination of core drill samples to map and characterize the dolerite dyke swarmstraversing the Kalamonmining permit.
Filteredanalysis of the total magneticfield (reduction to the pole, analytic signal, and first vertical derivative) revealsnarrow, highlymagneticlinear anomalies withpreferential N-S to NNE-SSW and NW-SE trends. Microscopicexaminationdemonstratesthatthese basic intrusions exhibit a typicalophitic to subophitic texture, dominated by interlocking plagioclase laths (labradorite to bytownite) and augite, accompanied by a significant proportion of iron-titanium oxides (titaniferousmagnetite and ilmenite), whichaccount for the high aeromagneticresponse. Low-grade deutericalterations are marked by partial uralitization of pyroxenes and sericitization of plagioclases. This integratedgeophysical and petrographicapproachproveshighly effective in reconstructingsubvolcanicmagmatic conduits and refining the regionalgeodynamicframework.

Keywords:*Aeromagnetics, Dykes, Petrography, Kalamon, Bouna, West African Craton.*

1. Introduction

In Precambrian cratons, and more particularlywithin the West African Craton, mafic dyke swarms (dolerites, gabbros, and sheetedbasalts) constitute premier geodynamic markers (Milési et al., 1989; Ernst *et al*., 2013). They reflect major episodes of lithospheric extension,

UNDER PEER REVIEW IN IJAR

oftenassociatedwith the breakup of supercontinents or the emplacement of large igneous provinces (LIPs) (Baratoux et al., 2011; Eglinger*et al*., 2017).

In northeastern Côte d'Ivoire, the Bouna region—and more specifically the Kalamonmining permit—ischaracterized by a Paleoproterozoicbasement (approximately 2.2–2.1 Ga) cut by multiple generations of brittle structures and dyke intrusions (Siagné*et al*., 2022). However, the geologicalstudy of theseBirimian structures isstronglyconstrained by advancedlateriticweathering, whichmaskslithological contacts and outcropcontinuity.

To overcomethesefieldconstraints, high-resolutionairbornegeophysics—particularlymagnetometry and gamma-ray spectrometry—constitutes a high-performing, non-destructive method for mapping lithological variations and the structural network beneath cover (Reford, 2006; Aïfa, 2021).

The main objective of thisworkis to combine the results of airbornegeophysicalprocessing and petrographic analyses under a polarizing microscope to establish the structural mapping, dyke geometry, and mineralogicalcharacterization of the dolerite dykes within the Kalamon permit.

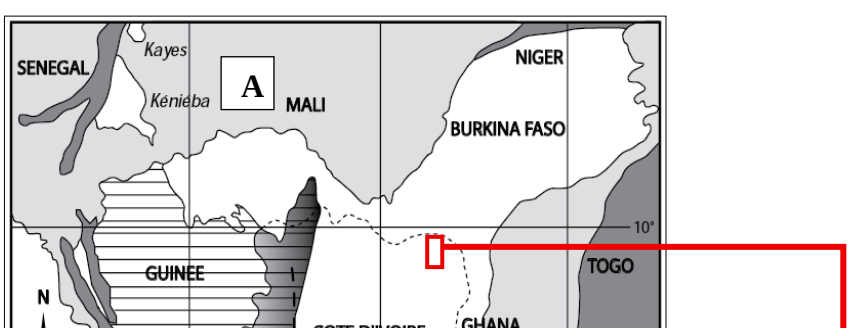
2. Regional and Local Geological Setting

The Kalamonmining permit issituated in the heart of the Paleoproterozoic Baoulé-Mossi domain (Fig. 1 A), whichformsmost of the eastern and central parts of the West African Craton in Côte d'Ivoire (Tagini, 1971 ;Bessoles, 1977). The architecture of thisPrecambrianbasementis the product of the Eburneanorogeny (2.2–2.0 Ga), characterized by major episodes of crustal accretion, subduction, and tectono-metamorphic collision (Boher et al., 1992 ;Feybesse et al., 2006 ;Baratoux et al., 2011).

On a regionalscale, this crystalline and crystallophyllianbasementismainlystructured by two major lithotectonic assemblages. On the one hand, the volcano-sedimentarygreenstonebelts (Birimian), formedbetween 2.15 and 2.10 Ga, comprise mafic lava sequencesdominated by tholeiiticbasalts, intermediate-to-fclsic flows, and volcano-sedimentarydeposits (detritalsediments and tuffs). Thesesequences have recordedpolyphaseregionalmetamorphismwith an intensitygenerallyrangingfrom green-schist to lower amphibolite facies (Hirdes et al., 1996 ; Lompo, 2009). On the other hand, the syn- to post-orogenicgranitoidplutonic complexes, whichintrude and frame thesegreenstonebelts, are dominated by tonalite-trondhjemite-granodiorite (TTG) suites as well as potassiccalc-alkaline granites (Kouamelan et al., 1997 ; Gasquet et al., 2003 ; Martin et al., 2005).

On a local scale, the Kalamon area ischaracterized by a heterogeneousgranitoidbasement (Fig. 1 B) dissected by a dense network of brittle to brittle-ductile faults and shear corridors with a preferential N-S to sub-N-S orientation. These zones of crustal weaknessplayed a key hydrogeological and structural role by acting as preferential conduits (drains) for the ascent and injection of latetholeiitic magmas, whichcrystallized as dolerite dyke swarms (Dadet, 1969 ;Siagné et al., 2022 ;Siagné et al., 2025).

Finally, the morphology and outcrop conditions of this area are stronglycontrolled by intense, prolongedsupergeneweatheringunder a humid tropical climate. This weatheringdynamicpromoted the development of a duricrust profile and a thickferruginous and bauxiticlateritic cover frequentlyreaching 50 to 90 meters in depth. This thickregolithalmostcompletelymaskslithological contacts at the surface, making the combined use of coredrilling and airbornegeophysicalimaging essential to accuratelyreconstruct the fine geometry of the geological structures.



UNDER PEER REVIEW IN IJAR

UNDER PEER REVIEW IN IJAR

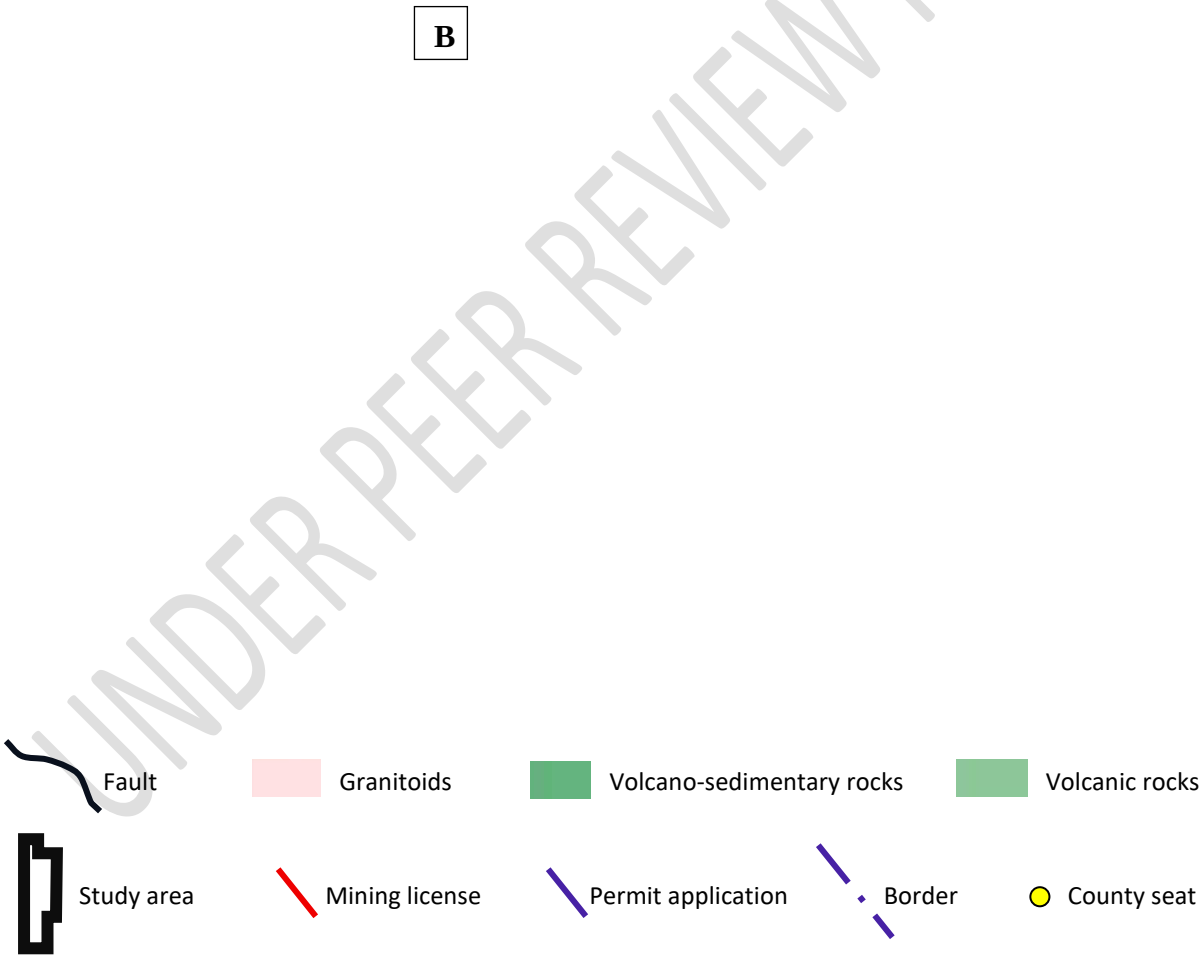


Figure 1 :(A) Map of the Man Rise (Bessoles, 1977 ; modified) and (B) Syntheticgeologicalmap of the Kalamonminingsector (CENTAMIN Report, 2017).

3. Methodology

3.1. Airbornegeophysics

Airbornegeophysicalsurveysconstitute a rapid, large-scale reconnaissance approach, particularlywell-suited for covering extensive areas prior to refining the interpretationthroughdetailed investigations. In thisstudy, the airbornesurveyswereconductedusing a magnetometer and a spectrometeronboard an aircraft, enabling the simultaneous acquisition of magneticfield variations and gamma-ray radioactivity. The airbornegeophysical data usedoriginatefrom a high-resolutionregionalsurveyacquiredalong flight linesspaced 200 m apart, with a sampling interval of 5 m along profiles and a nominal flight height set at 80 m.**3-**

3.1.1. Magnetism

The magneticmethodmeasures spatial variations in the intensity of Earth'smagneticfield, which are influenced by global contributions from the core and mantle as well as magneticsusceptibilitycontrasts of local geological bodies. Measurementswerecollectedusing a cesiumvapormagnetometerfeaturing a sampling rate of 0.1 seconds and a high resolution of 0.01 nT. Raw data processingrequiredapplying the Reduction to the Pole (RTP) correction to position magnetic anomalies directlyabovetheirgeological sources by overcoming local inclination effects. To optimize structural and lithological mapping, additionalenhancementswereapplied, including the first vertical derivative (1VD), which highlights vertical gradients and sharpens the boundaries of geological bodies and subvertical contacts, and the analytical signal (AS), which simplifies magnetic source geometry by generating positive anomalies centered over inductive bodies.

3.1.2. Radiometry (RAD)

Airborne gamma-ray spectrometrymaps the superficial distribution of naturalradioelements (potassium [K], thorium [Th], and uranium [U]). The equipmentincluded a spectrometerequippedwith thallium-activated sodium iodide (NaI) crystals capable of measuringenergyspectraassociatedwith the radioactive decay of these tracer elements.

3.2. Ground Validation and Petrographic Analyses

The interpretation of geophysical data wasvalidated by a rigorousfieldcampaignrelying on referencecartographic documents. Due to the thicksupergeneweathering cover (reaching 50 to 90 m in thicknessdepending on the sector), direct surface observations werecomplemented and supplemented by the systematicanalysis of coreboreholes.

Sample selectionwasbased on a meticulousanalysis of lithological logs in order to select the freshest, mosthomogeneous, and representative facies reflectinglateral and vertical continuity. A total of around one hundredsampleswerecollected in compliance withgeologicalsafety standards. The positions of outcrops and boreholesweregeolocatedusing a Garmin Etrex GPS receiver.

The petrographic and mineralogicalstudybeganwith a macroscopicvisual description of the various lithologies beforeproceeding to microscopicanalysisusing a polarizing microscope. The latter relied on the examination of about twentythin sections, prepared in part at the University of Paris XI (France) and at the Analysis and Research Center (CAR) of the Petroleum Operations Company of Côte d'Ivoire (PETROCI). All of thesemacroscopic and microscopic descriptions werecarried out at the Laboratory of Geology, MineralResources, and Energy of the UFR of Earth Sciences and MineralResources at Université Félix Houphouët-Boigny in Abidjan-Cocody. Additionally, the magneticsusceptibility of the sampleswasmeasuredusing a KT-10 magneticsusceptibilitymeterfrom Terra Plus (Fig. 2).



UNDER PEER REVIEW IN IJAR

Figure 2 : KT-10 Magnetic Susceptibility Meter.

3.3. Computer Processing and Cartographic

Integration The computationalmethodologyrelied on the multi-layer integration of geophysical data (magnetism and radiometry) and geological mapping using the Quantum GIS (QGIS) Geographic Information System. The extraction of lineamentsfrom the 1VD aeromagneticgeophysical image enabled the generation of a detailedmagneticdiscontinuitymap. In contrast, major lineamentswerehighlightedusingreduced-to-the-pole (RTP) magnetic data. Measurementswereplotted on stereogramsusingGeorient software.

Existing 1:200,000 geological and 1:50,000 topographicmapsweregeoreferenced in the UTM projection system (Zone 30N, WGS 84 Datum). Applying a cross-transparency (around 50%) between the aeromagnetic and radiometricsurvey images superimposed on the base mapallowed for the generation of composite maps. This synopticvisualapproachgreatlyfacilitates the identification of major structural lineaments, hiddenfaults, and major lithological contacts masked by the lateritic cover.

4. Results

4.1. Geological Mapping

The cross-referencing of airbornemagneticgeophysical data withanalytical signal processing (MAG-AS), radiometric data (RAD) (Fig. 3), and fieldlithological data (Figs. 4 and 5) enabled us to observe three distinct petrographicallydefinedunitsthat are unevenlydistributedacross the entireKalamon permit (Fig. 6).

UNDER PEER REVIEW IN IJAR

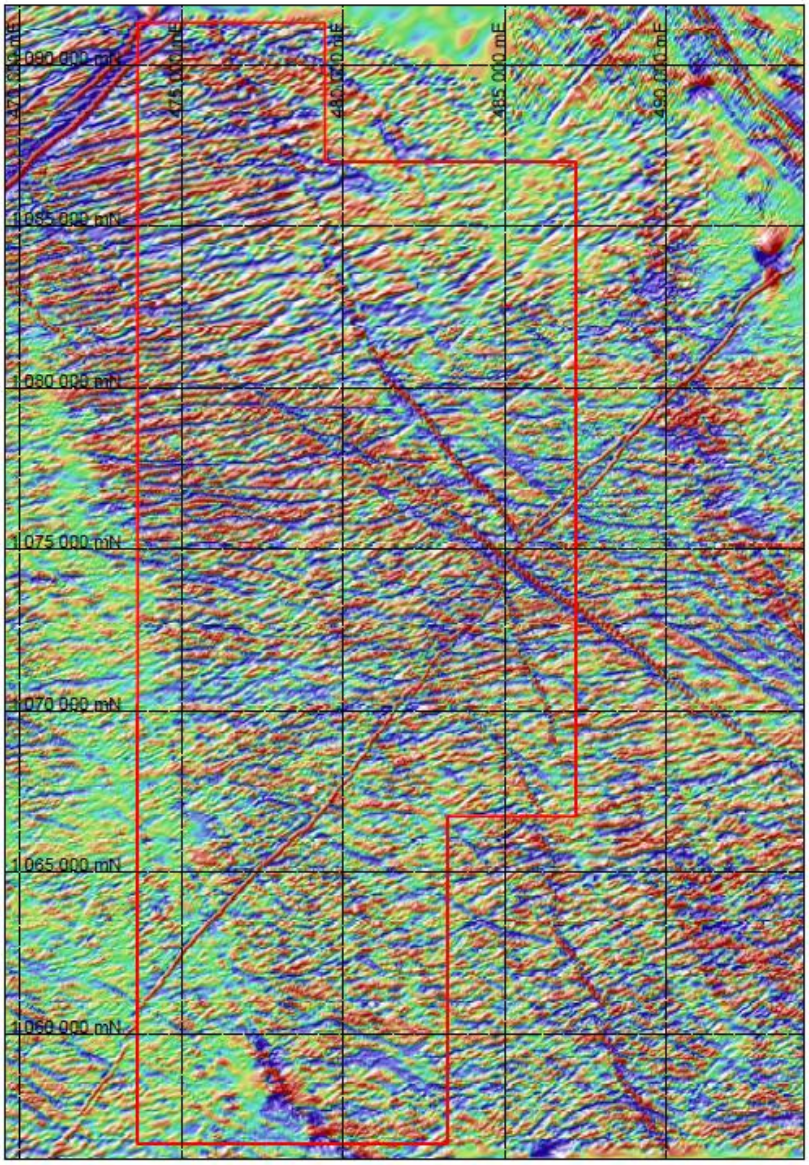


Figure 3 :1VD-RTP TMI GeophysicalMap.

4.1.1. Unit I (Undeformed Granodiorite)

This unit, or Type I granodiorite, composed of undeformed or weaklydeformed granodiorite, displays a slightly rough texture on the geophysical image, withmagneticsusceptibilitiesrangingfrom 1.89 to 3.84 × 10^{-3} SI and a densityvaryingfrom 2.54 to 2.74 × 10^{3} kg/m^{3}, appearing in a yellowish-green tone (Table I). It appears to be in sharp contact with Unit II.

In the Kalamonsector, undeformed granodiorites constitute a significant portion of the plutonic complexes. At the macroscopicscale, these rocks present a massive, mesocratic aspect with a pinkish or whitishtendency, possessing a medium- to coarse-grainedgranular texture. They display a visible mineralogydominated by translucent quartz, abundant feldspaths (plagioclases and potassium feldspaths), as well as disseminated biotite flakes (Fig. 4 A).

Microscopicexaminationunderpolarized light accuratelycharacterizes the primarymineralparagenesis and the deutericalteration stages affectingthesefacies :

- Quartz : It represents 35 to 45% of the rock and occurs as large xenomorphiccrystalswithlobedboundaries, as well as clusters of interstitial micro-grains. The quartz frequentlyexhibitspronouncedundulatory extinction, reflecting post-crystallizationtectonic stresses experienced by the basement (Fig. 4 B).

- Potassium feldspaths :Largelydominated by orthoclase and microcline, theyconstitute 25 to 30% of the mineralogical volume. They manifest as large subhedralphenoblastssometimesdisplaying Carlsbad twinning or a fine perthite network (albite exsolution), and are moderatelyaltered by sericitization (Fig. 4 B).
- Plagioclases : More discreetthan in the granodiorites, theyrepresent 15 to 20% of the rock. Of sodic composition (oligoclase to albite), theyoccur as subhedrallathsshowingpolysynthetic albite twinsoftenblunted by secondaryalteration (Fig. 4 B). A fine albiticrim or discrete zoning isfrequentlyobserved.
- Biotite : The main yetsparseferromagnesian phase (3 to 6%), itoccurs as fine subhedrallamellae of brown to greenishcolor, affected by partial chloritization. It contains zircon inclusions characterized by darkpleochroichaloes (Fig. 4 B).
- Accessory and secondaryminerals: The accessory assemblage includes rare crystals of sphene, apatite, and disseminated opaque oxides. Low-grade hydrothermal alteration phases result in the development of sercite at the core of feldspaths, chlorite at the expense of biotite, and epidotemicrocrystalsscatteredthroughout the matrix (Fig. 4 B).

4.1.2. Unit II (Deformed Granodiorite)

It corresponds to the most extensive and dominant lithological unit of the Kalamon permit. This unit, corresponding to deformed or Type II granodiorites, exhibits a rough texture on the geophysical image, with a magneticsusceptibilityrangingfrom 1.30 to 9.76 × 10^{-3} SI and a densityvaryingfrom 2.54 to 2.69 × 10^{3} kg/m^{3}. It appears in a red-to-dark-blue coloration associatedwithhaloedyellow to sky-bluetones (Table I). This unit appears to intrude Unit I. The images indicate an unusual abrupt change between Unit II and Unit I, whichundoubtedly corresponds to a lithological contact.

Macroscopically, the granodiorites have a medium- to coarse-grainedgranular texture, darkermesocraticthanthat of Unit I, with a massive appearance. It ismainlycomposed of feldspars and quartz in variable proportions. Theseminerals are associatedwith biotite and amphibole, also in variable proportions (Fig. 4 C).

From a microscopicstandpoint, the followingminerals are observed:

- Plagioclases : They are the mostwidelyrepresentedminerals (approximately 45 to 50%). The plagioclases are of highly variable size, euhedral, and altered. They exhibitpolysynthetictwinsoftenobliterated by alteration. The plagioclases present large, slightlysericitized areas (Fig. 4 D). Some plagioclases are zonedwith a generallyalteredcalciccore and a more or lessclearalbiticrim.
- Quartz : Quartz reaches proportions of 30 to 35% of the rock. It occurs as globularcrystals and xenomorphic areas. This mineral displays highly variable sizes rangingfrom micro-grain to coarse grain withremarkableundulatory extinction (Fig. 4 D).
- Biotite :Accounting for 10 to 15%, biotite occurs as subhedral to euhedrallamellae, brown in colorturningsometimes to light green, undoubtedly due to chloritization. It displays direct pleochroism. A few zircon inclusions surrounded by a dark halo are alsoobserved (Fig. 4 D).

4.1.3. Unit III (Dolerite Dykes)

This unit, the youngest, corresponds to intermediate rock dykes cuttingacross the previousunits. Theirmagneticsusceptibilitiesvaryfrom 2.11 to 7.18 × 10^{-3} SI (strongresponse) with a densityvaryingfrom 2.56 to 2.99 × 10^{3} kg/m^{3}. They appear in a red coloration (Table I).

Macroscopically, the Kalamondolerites are dark, melanocratic to mesocratic rocks, very dense and littlealtered at depth (Fig. 5 A).

Under the microscope, the rocks display a remarkableophitic to subophitictexture :

- Plagioclases : They form (45–55%) entangledeuhedrallathsshowingpolysynthetic albite twinning. They are moderatelyaffected by sericitization (Fig. 5 B).
- Pyroxenes: Representedpredominantly by colorless to slightlygreenish augite (30–40%), occupying the interstitialspacesbetween plagioclase laths. Some crystals show borderstransformedinto actinolite/tremolite (uralitization) (Fig. 5 B).
- Opaque minerals: They appear as disseminatedskeletal or idioblastic grains (5–10%). Reflected-light analysisconfirms the predominance of titaniferousmagnetite and ilmenite. It isthis high content of magnetic opaque mineralsthatexplains the intense signature observed on airbornesurveys (Fig. 5 B).
- Accessory and secondaryminerals: Traces of apatite, lateinterstitial quartz, chlorite, and epidoteassociatedwith hydrothermal-deutericalteration.

UNDER PEER REVIEW IN IJAR

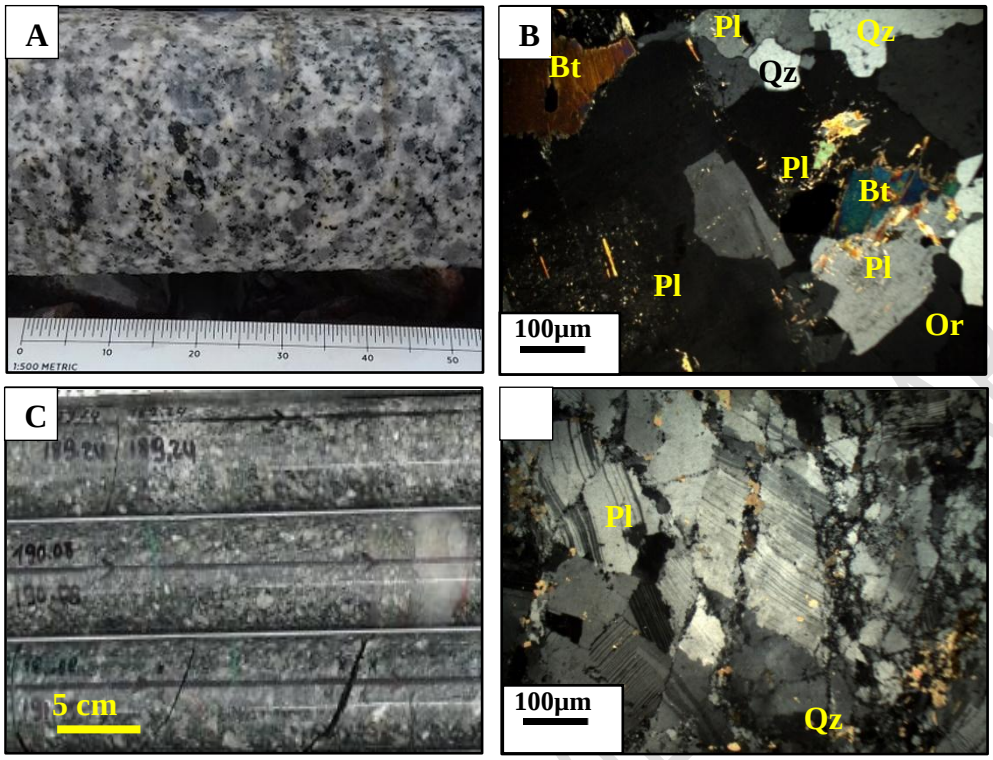


Figure 4 : Macroscopic aspects and photomicrograph of a granodiorite.
A : Granite coresample **;B :**Photomicrograph of the granite**.**
Pl : plagioclase ; Qz : quartz ; Or : orthoclase ; Bt : biotite ; Hbl : green hornblende ; Ep : epidote; Ser : sericite

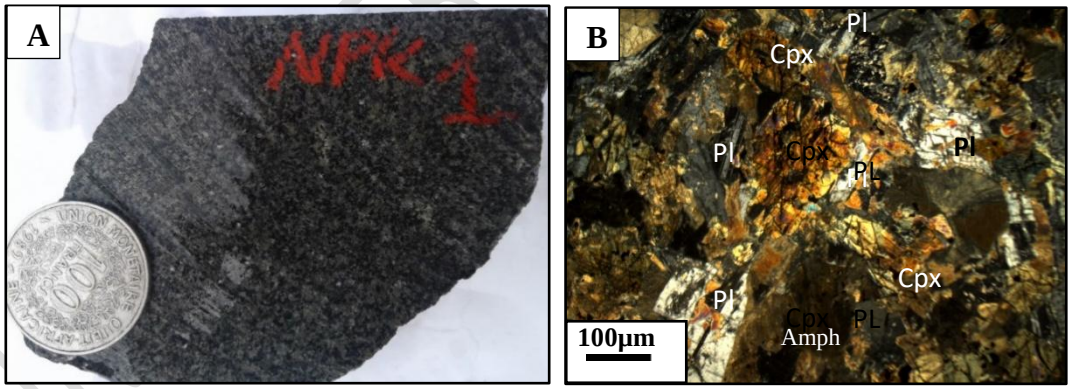
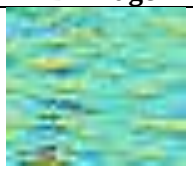
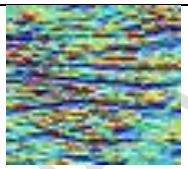
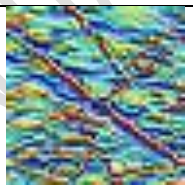


Figure 5 : Macroscopic aspect and photomicrograph of a dolerite.
A : Macroscopic aspect of a dolerite ; **B :** Photomicrograph of the diorite.
Pl : plagioclase ; Cpx: clinopyroxene ; Bt: biotite ; Amph: amphibole ; Op : opaque mineral

Table I : Characteristiccolor set for lithologies.

Unit	Lithology	Magnetic Susceptibility (SI)	Characteristics	TMI 1VD-RTP + RAD Image
I	Undeformed Granodiorite	1,89 et 3,84 10^{-3}	- Slightly rough texture - Low magneticresponse	
II	Deformed Granodiorite	1,30-9,76 10^{-3}	- Strongly rough texture - High magneticresponse	
III	Dolerite Dykes	2,11-7,18 10^{-3}	- Linear structure - High magneticresponse	

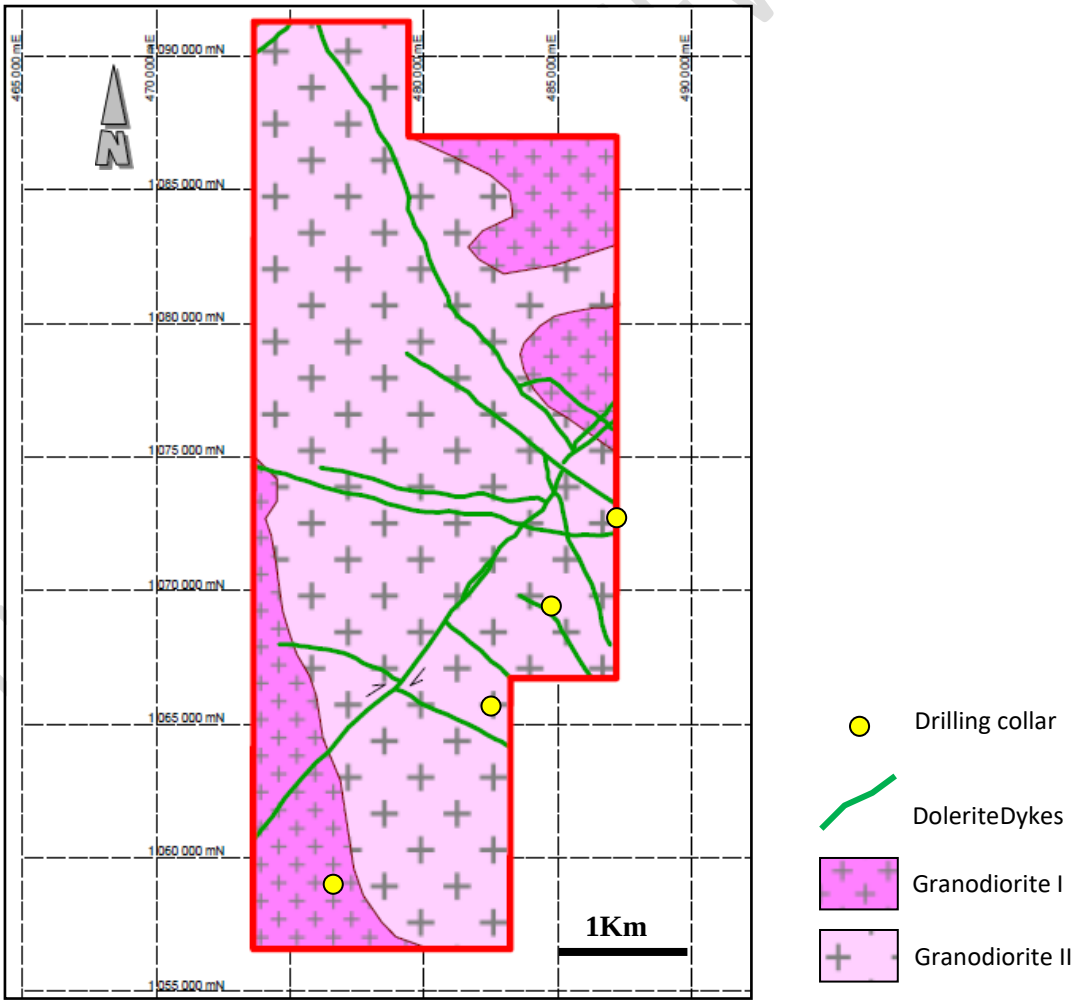


Figure 6 : Geological sketch of the study area based on geophysical and field data.

4.2. Structural Analysis

Visual and manualinterpretations of the geophysical images (Fig. 7) enabled us to obtain a lineamentmap (Fig. 8). This mapping wascomplemented by studiescarried out on drill cores, whichallowed us to identifyseveralfamilies of lineaments.

4.2.1. LineamentMap

The lineament data maps (Fig. 7) generally show linear structures, commonlyinterpreted in granitoids as related to fracturing, jointing, foliation, banding, or schistosity.
The extractedlineaments (Fig. 8) vary in lengthfrom the metric to the plurikilometricscale. Their distribution across the image followsseveral orientations. Statisticalanalysis of the lineamentsrevealsthree major families of lineament orientations. Based on the number of lineamentsextractedfrom the 1VD-RTP TMI image and discriminated by a thresholdgreaterthan 10%, we can observe on the directional rose diagram (Fig. 9) that the NE–SW lineament class rangingbetween [N30°–N70°] is the mostabundant. The second directional class is the NW–SE direction, represented by the [N110°–N130°] class. Finally, the thirdlineament class isgloballyoriented E–W [N080°–N100°]. Indeed, the major NE, NW, and E–W lineamentsdefine a fracture system resulting from ductile-brittledeformation.

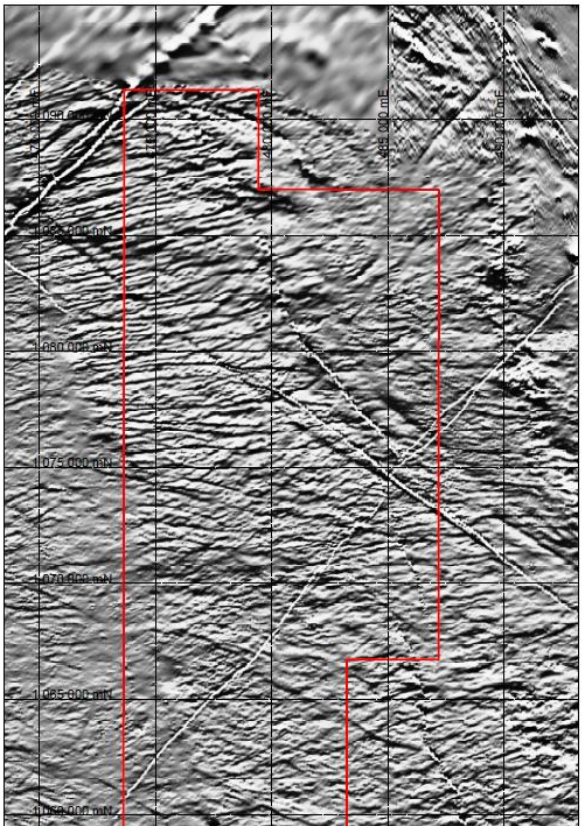


Figure 7 :TMI 1VD-RTP image showinglineaments.

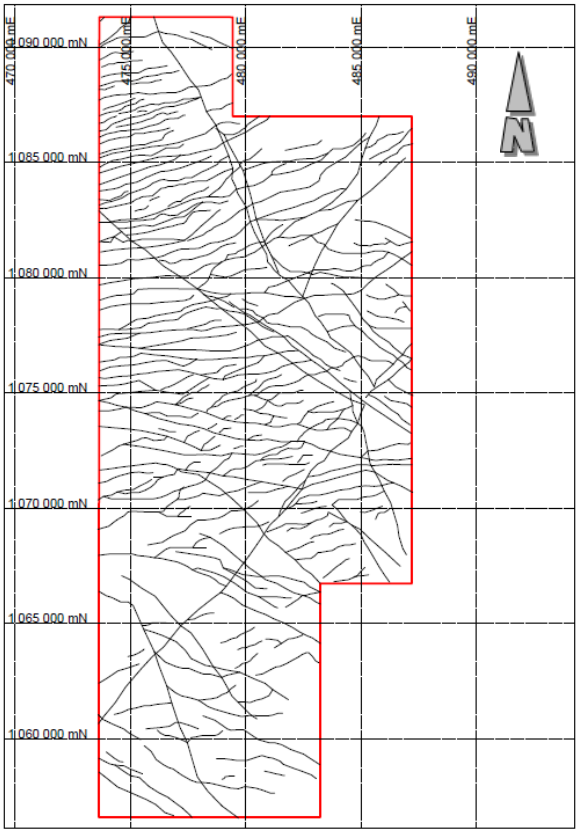


Figure 8 :Lineament network map.

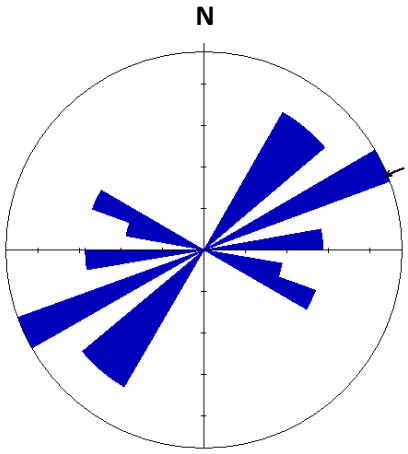


Figure 9 : Directional rose diagram of lineaments.

4.2.2. Ground Work Validation

4.2.2.1. Outcrop Observations

In the field, structural elementswere difficult to measure due to intense weathering, whichrendersoutcropsnearly invisible. Nevertheless, wewere able to take a few measurements (Fig. 10) thatconfirm structures belonging to the [N120°–N130°] directional class.

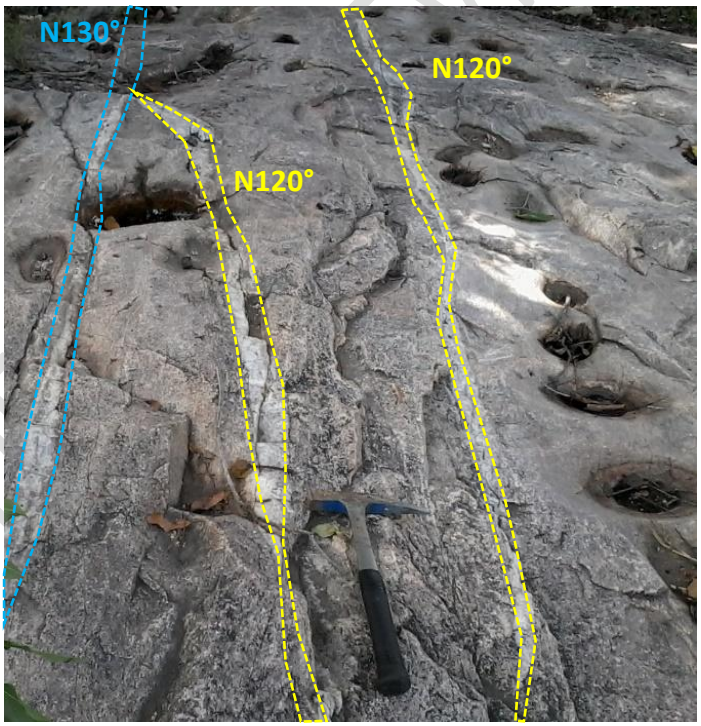


Figure 10 : Photographillustrating a granite outcropwith N130°-trending fractures filledwithmilky quartz.

UNDER REVIEW IN IJAR

4.2.2.2. On Drill Cores

Diamond drillingcampaignsalsointersected type I and II granodiorites as well as dolerite dykes. Severalfamilies of mesostructureswereidentified on the drill cores. These structures resultfrombrittletectonics and consist of quartz veins and veinlets, as well as fractures.

- Veins and Veinlets

Quartz veins can begroupedintoseveralfamilieswithspecificgeometriccharacteristics (thickness, strike, and dip). The veins range in thicknessfrom a few centimeters to severalmeters. As for veinlets, whosethicknessislessthan 1 cm, they are predominant in the study area. They constitute a true network of fractures filledwith quartz crystals (Fig. 11 A), sometimesassociatedwith calcite, but they can alsobeinfilledwith chlorite, epidote, and hematite. Measurementscarried out on these structures revealthatthey are pluridirectional (Fig. 11 B). Nevertheless, three main orientations emerge:

  - NW–SE with dips toward the SW (mean plane N130°, 45°SW);
  - NE–SW with dips toward the NW (mean plane N40°, 35°NW); and
  - the presence of sub-meridian N–S veins (mean plane N5°, 10°NW).

- Fractures

Fractures (*sensu stricto*) are widelyobserved in the cores (Fig. 11 C). These fractures are pluridirectional (Fig. 11 D) and crosscut the entire rock mass. Most measurementsyield the following orientations:

  - NE–SW dippingtoward the NW (mean plane N60°, 50°NW);
  - N–S dippingtoward the W (54°W);
  - E–W dippingtoward the SW (mean plane N280°, 35°NW).

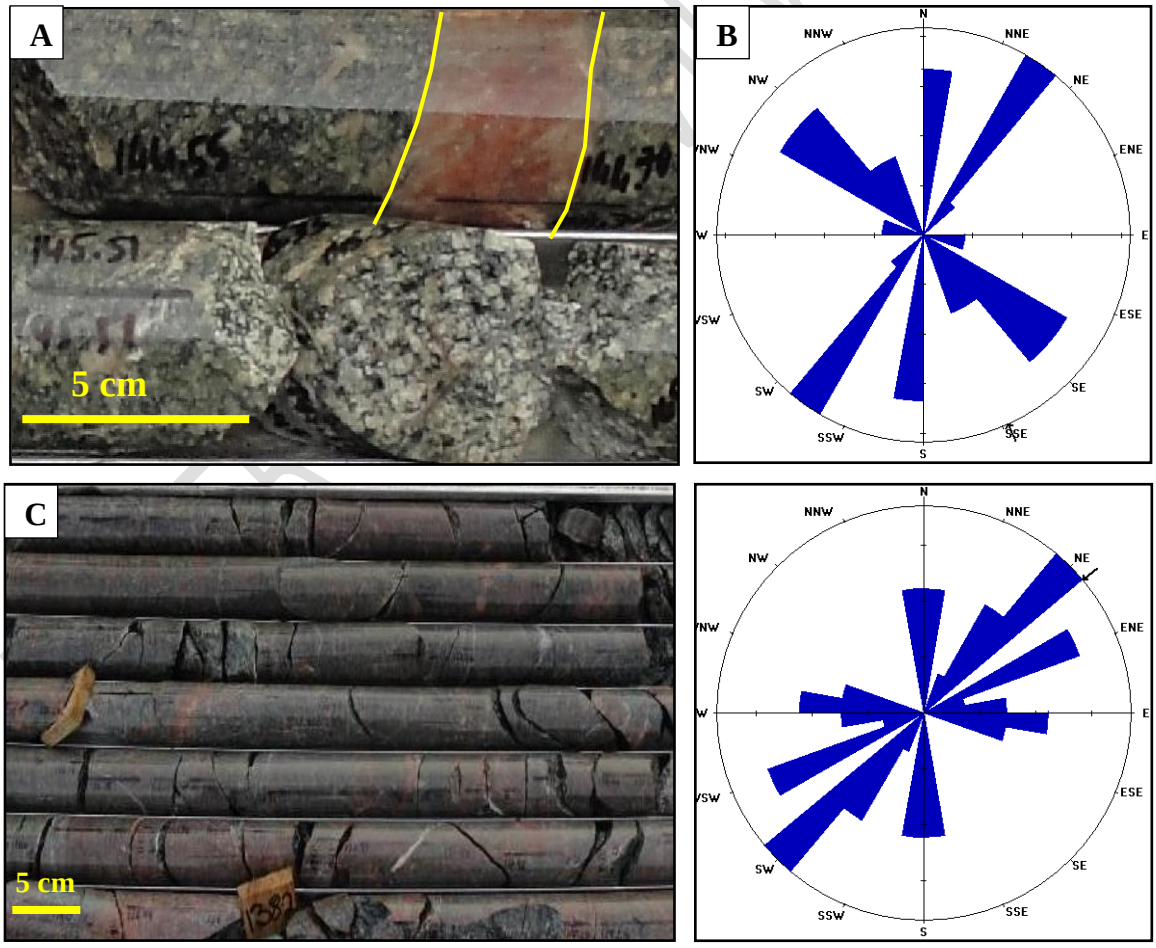


Figure 11 : Rose diagrams and photographs of some structures observed on drill core.

A : Directional rose diagram of quartz veins; **B :** Photograph of a quartz vein**; C :** Directional rose diagram of fractures ; **D :** Photograph of fractures**.**

5. Discussion

5.1. Integration of Geophysical and Petrographic Data : Origin of Magnetic Signatures

Combiningairbornegeophysicalimaging data (TMI 1VD-RTP and Analytic Signal) withpetrographic and lithological observations highlights a close correlationbetweenmagneticsusceptibilitycontrasts and the nature of the intrusive facies.

The undeformed granodiorites (Unit I) are characterized by a weak to moderatemagneticresponse and a slightly rough texture. Mineralogically, thisisexplained by the abundance of felsic silicate phases (quartz and feldsparstotaling over 75–80%) and the scarcity of primaryiron oxides, with biotite and green hornblende constituting the bulk of the ferromagnesianminerals.

In contrast, the deformed Type II granodiorites and especially the dolerite dykes (Unit III) are distinguished by sharp, high-amplitude internalmagnetic anomalies and a strongly rough texture. Micrographicexamination of the doleritesdemonstratesthatthis high magneticintensityisdirectlylinked to the presence of 5% to 10% primary opaque minerals, dominated by titaniferousmagnetite and ilmenitedisseminatedwithin an ophitic to subophitic texture matrix (augite and plagioclase). These observations corroborate the works of Reford (2006) and Airo &Loukola-Ruskeeniemi (2004), whoemphasizethatmagneticsusceptibility variations in crystalline basements are primarilygoverned by the distribution of opaque oxides and deutericalterationparageneses (uralitization and saussuritisation).

5.2. Structural Control and Kinematics of Magmatic Intrusions

Statisticalanalysis of the lineamentsextractedfrom the TMI 1VD-RTP image and the rose diagram (Fig. 9) reveal major structuringdominated by the N120°–N130° direction, composed of secondaryfamiliesoriented N080°–N100° and N030°–N040°.

Although the thicksupergeneweathering cover (oftenexceeding 50 meters) almostentirelymasks surface outcropsa classicconstraintdocumented in the West Africanbasement (Tagini, 1971 ;Bessoles, 1977), validation by diamonddrilling and rare field observations (multimeter-scale N130°-trending fractures filledwithmilky quartz) confirm the primaryrole of thesetectonic corridors.

These fracture families and shear zones constitute major crustal structures inheritedfrom the Eburneanorogeny. They acted as preferentialhydrogeological and magmaticpathways, favoring on the one hand the ascent and late emplacement of Type II granites, and on the other hand the subsequent injection of tholeiitic magmas as dolerite dykes (Dadet, 1969 ;Siagné et al., 2022 ;Siagné et al., 2025). This brittle to brittle-ductile tectonicregimereflects a classic post-orogenicextensional or transtensional setting in the geodynamicevolution of the West African Craton (Dumont et al., 1997 ; Ernst et al., 2013).

The petrological association observed in the Kalamonsector, combining an intrusive granodioriticbasement and a lateswarm of intermediate dykes, fitsharmoniouslyinto the regionalgeodynamicframework of the Paleoproterozoic Baoulé-Mossi domain (Boher et al., 1992 ;Feybesse et al., 2006). On a regionalscale in Côte d'Ivoire, the Kalamon Type I and II granodiorites sharestrongpetrographicaffinitieswithplutonic complexes described in otherIvoriangreenstonebelts, such as Fettékro, Oumé, or Dabakala (Doumbia et al., 1998 ;Gnanzou, 2014 ;Allibro et al., 2014). In thiscontext, the presence of amphibole phases (green hornblende) and biotite affected by low-grade hydrothermal alteration (chloritization, epidotization, and sericitization) constitutes a ubiquitousfeature of peri-intrusive halos and mineralized corridors of the IvorianBirimian (Milési et al., 1989 ; Kouadio et al., 2023). Finally, across the West African Craton scale, the N120°- and N–S-orienteddolerite dyke swarmscrosscutting the Eburneangranitoidsreflectregionallithosphericfracturing phases comparable to thoserecognized in Burkina Faso (Lompo, 2009 ; Vidal et al., 2009) and Ghana (Hirdes et al., 1996 ; Allibone et al., 2002). These basic intrusions generallyseal the end of the major tectono-metamorphicparoxysms of the Eburneanorogeny (2.1–2.0 Ga) and bearwitness to major continental extensionaleventspreceding the final stabilization of the craton (Baratoux et al., 2011 ;Eglinger et al., 2017).

6. Conclusion

This studycarried out on the Kalamonmining permit (Bouna region, northeastern Côte d'Ivoire) demonstrates the efficiency and relevance of the methodologicalapproachcoupling high-resolutionairbornegeophysicalimaging and in-depthpetrographicanalysis on drill cores.

In a Paleoproterozoicbasementcontextheavilymasked by a thicksupergeneweathering cover (laterites and saprolitesreachingdepths of 50 to 90 meters), aeromagnetic data processing—

UNDER PEER REVIEW IN IJAR

includingReduction to the Pole (RTP), the First Vertical Derivative (1VD), and Analytic Signal (AS)—overcamefieldconstraints to map the structural architecture and spatial footprint of mafic dyke swarmswithunprecedentedprecision.

Petrographic and mineralogical investigations characterizedthese intrusions as doleriteswith an ophitic to subophitic texture, dominated by the association of calcic plagioclases (labradorite to bytownite) and clinopyroxenes (augite), supplemented by a significant proportion of primary opaque minerals (titaniferousmagnetite and ilmenite). It ispreciselythisabundance of iron-titanium oxides that justifies the intense linearmagnetic signature recorded by the airbornesurveys.

Structurally, statisticalanalysis of lineaments and major directions highlights rigoroustectonic control characterized by fault and dyke familieswith dominant N–S to NNE–SSW and NW–SE orientations (with a markedrelayrepresented by the N120°–130° class). These crustal weakness corridors, inheritedfrom the Eburneanorogeny, acted as major magmatic conduits during post-orogenicextensional phases. This dynamicfitsperfectlyinto the regionalgeodynamicframework of the Baoulé-Mossi domain and the West African Craton, confirming the strategicinterest of thesemagmatic markers for understanding the Precambrianlithosphere.

7. References

Aïfa, T. (2021). Geophysics and geodynamics of West African Craton. *Journal of African Earth Sciences*, 175, 104120.

Airo, M. L., &Loukola-Ruskeeniemi, K. (2004). Characterization of geologicalmaterials by magnetic and petrophysicalproperties: Application to ore exploration in Fennoscandia. *Geological Survey of Finland, Special Paper*, 37, 33–45.

Allibone, A., McCuaig, T. C., Harris, D., Etheridge, M., Munroe, S., Byrne, D., & Blenkinsop, J. (2002). Lower Proterozoic gold deposits in the Ashanti Belt, Ghana :Geochronologicalconstraints. *EconomicGeology*, 97(3), 505–517.

Allibro, A., Kouamé, F., & Yao, B. J. (2014). Pétrographie et contexte géodynamique des granitoïdes de la région de Dabakala (Nord-Est de la Côte d'Ivoire). *Journal des Sciences Géologiques et Appliquées*, 12(2), 45–60.

Baratoux, L., Jessell, M. W., Feybesse, J. L., Ilboudo, H., & Cottereau, N. (2011). Initiation and paleoproterozoicaccretion of the West African Craton. *PrecambrianResearch*, 187(3-4), 169–199.

Bessoles, B. (1977). *Géologie de l'Afrique : le Craton Ouest-Africain*. Mémoires du BRGM, n° 88, Paris, 383 p.

Boher, M., Abouchami, W., Michard, A., Albarède, F., & Arndt, N. T. (1992). Crustal growth in West Africa at 2.1 Ga. *Journal of GeophysicalResearch*, 97(B1), 345–369.

CENTAMIN (2017) : Rapport technique de decembre 2017 du projet de Kalamon, Côte d'Ivoire, 20 p.

Dadet, P. (1969). *Notice explicative de la carte géologique de la République de Côte d'Ivoire au 1/500 000*. SODEMI, Abidjan, 145 p.

Doumbia, S., Yao, B. J., Tagini, B., & Kouamé, F. (1998). Le magmatisme paléoprotérozoïque du sillon de Fettékro. *Journal of African Earth Sciences*, 27(3), 345–362.

Dumont, J. F., Poupinet, G., & Soule, J. C. (1997). Late Eburnean tectonicevolution of the West African Craton in Côte d'Ivoire. *PrecambrianResearch*, 84(1-2), 45–65.

Eglinger, A., Bari, A., Robb, L. J., Augenstine, M., & Zeh, A. (2017). Paleoproterozoic crustal evolution and gold metallogeny of the West African Craton. *Ore GeologyReviews*, 81, 1050–1068.

Ernst, R. E., Bleeker, W., Söderlund, U., & Kerr, A. C. (2013). Giant dyke swarms and mantle plumes: Implications for continental breakup. *Geological Society, London, Special Publications*, 382(1), 1–45.

Feybesse, J. L., Billa, M., Guerrot, C., Duguey, E., Lescuyer, J. L., Milési, J. P., & Bouchot, V. (2006). The Paleoproterozoic of the West African Craton: A synthesis. *PrecambrianResearch*, 149(3-4), 127–154.

Gasquet, D., Barbey, P., Adou, M., & Paquette, J. L. (2003). Geochronology, geochemistry and geodynamicsignificance of a Paleoproterozoic continental margin in the Baoulé-Mossi domain (West African Craton, Ivory Coast). *PrecambrianResearch*, 127(4), 313–329.

UNDER PEER REVIEW IN IJAR

Gnanzou, A. (2014). *Étude pétrographique et géochimique des granitoïdes de la région de Dabakala*. Thèse de Doctorat, Université Félix Houphouët-Boigny, Abidjan, 210 p.
Hirdes, W., Davis, D. W., & Lüdtke, G. (1996). Two-stage Birimian (Paleoproterozoic) volcanism and plutonism in the West African Craton (Ghana) and theirgeodynamicsignificance. *PrecambrianResearch*, 80(3-4), 173–192.
Kouadio, K. J., Allou, Y., & Ouattara, A. S. (2023). Hydrothermal alteration and fluidevolution in Paleoproterozoic gold deposits of West Africa. *Journal of African Earth Sciences*, 198, 104780.
Kouamelan, A. N., Deloule, E., &Peucat, J. J. (1997). Geochronological and geochemicalconstraints on the Paleoproterozoicgeologicalevolution of the Haute Côte d'Ivoire. *PrecambrianResearch*, 85(3-4), 183–202.
Lompo, M. (2009). Geodynamicevolution of the PaleoproterozoicBirimian formations of the Liptako-Gourma region (Eastern Burkina Faso). *Journal of African Earth Sciences*, 53(1-2), 45–60.
Martin, H., Smithies, R. H., Rapp, R., Moyen, J. F., & Champion, D. (2005). An overview of adakite, tonalite-trondhjemite-granodiorite (TTG) and sanukitoid: relationships and some implications for crustal evolution. *Lithos*, 79(1-2), 1–24.
Milési, J. P., Feybesse, J. L., Ledru, P., Dommanget, A., Marcoux, E., Egal, E., & Calvez, J. Y. (1989). Les minéralisations d'or du Birimien (Protérozoïque inférieur) de l'Afrique de l'Ouest. Ses relations avec l'évolution lithostructurale et géodynamique. *Chronique de la Recherche Minière*, 497, 3–58.
Reford, S. W. (2006). Airbornemagnetic and gravity applications in mineral exploration. *Geophysics*, 71(6), G33–G47.
Siagné, Z. H., Ouattara, A. S., Konan, N. J. J., & Kouamé, F. (2022). New LithostructuralMap of the DoropoRegion, Northeast Côte d'Ivoire : Insight from Structural and Aeromagnetic Data. *Journal of African Earth Sciences*, 196, 104680.
Siagné, Z. H., Ouattara, A. S., & Allou, Y. (2025). Integration of airborne gamma-ray spectrometry and remotesensing data for mapping of gold-bearing structures in the Doroporegion, Northeastern Côte d'Ivoire. *Geocarto International*, 40(1), 2465074.
Tagini, B. (1971). *Esquisse géologique de la Côte d'Ivoire : son rôle dans la structure géologique de l'Afrique de l'Ouest*. Thèse de Doctorat, Univ. de Lausanne, 302 p.
Vidal, M., Deloule, E., Baratoux, L., & Jessell, M. W. (2009). Geodynamicevolution of the Birimian formations in Burkina Faso. *PrecambrianResearch*, 172(1-2), 110–128.

UNDER PEER REVIEW IN IJAR